Grain Growth Prediction of SS316L Stainless Steel of Bead-On-Plate Using Numerical Computation

Muhd Faiz Mat, Yupiter H. P. Manurung, Norasiah Muhammad, Siti Nursyahirah Ahmad, Mohd Shahriman Adenan, and Martin Leitner

Abstract In this study, the austenitic grain size in bead-on-plate heat-affected zone (HAZ) are predicted as grain size has been widely known as an important factor affecting the deformation mechanism of materials, its microstructures and mechanical properties. At the first stage, a numerical model of bead-on-plate process using Goldak's double ellipsoid heat source model is used to assess the temperature distribution during and after welding of austenitic stainless steel SS316L filler wire and plate. The numerical computation is conducted based on temperature-dependant materials properties using commercial FEM software MSC Marc/Mentat with user subroutine. Further, a numerical model is developed by using ordinary differential equation (ODE) for calculating the free grain growth algorithm combined with the presence of growing precipitates. The initial grain size (D_0) value was obtained from optical microscopy observation while other values such as modified kinetic constant (M_0) and activation energy (Q_a) are defined through experimental investigation with various temperature ranges and holding times. It can be concluded that the austenite grain growth prediction algorithm during the bead-on-plate welding thermal cycle was successfully executed. As the outcome, grain sizes were predicted and compared with experimental investigation.

Keywords Grain growth · Bead-on-plate · Austenitic stainless steel · ss316l

M. F. Mat · S. N. Ahmad
Faculty of Mechanical Engineering, Universiti Teknologi MARA (UiTM), 40450 Shah Alam, Selangor, Malaysia

Y. H. P. Manurung (✉) · M. S. Adenan
Smart Manufacturing Research Institute (SMRI), Universiti Teknologi MARA, (UiTM) 40450, Shah Alam, Selangor, Malaysia
e-mail: yupiter.manurung@uitm.edu.my

N. Muhammad
Jabatan Kejuruteraan Mekanikal, Politeknik Premier Sultan Salahuddin Abdul Aziz Shah, 40150 Shah Alam, Selangor, Malaysia

M. Leitner
Chair of Mechanical Engineering, Montanuniversität Leoben, 8700 Leoben, Austria

Recent Trends in Manufacturing and Materials Towards Industry 4.0,
Lecture Notes in Mechanical Engineering,
https://doi.org/10.1007/978-981-15-9505-9_1

1 Introduction

The microstructure and mechanical properties of the heat-affected zone (HAZ) of welded metal is significantly affected by the continuous welding heat input. This will affect the grain structure that affects the strength, toughness, ductility and corrosion resistance of the alloys [1]. The high operating temperature leads to change of grain size. Therefore, the attempt to predict the grain size is crucial to evaluate the effect of grain growth to degree of sensitization (DOS) as the inverse co-relationship of grain size and DOS was conclude in [2]. The modelling of the microstructural changes within the welded parts are the upmost important for engineers to save time and cost of fabrication. It should be noted that certain software, based on thermal and metallurgical modelling have been developed to predict the grain size at HAZ's in multipass welding and their effects on mechanical properties. The objective is to predict the changes in the material properties especially the grain size and if applicable used the numerical simulation for additive manufacturing application. Thus, it is important to distinguish the temperature-dependant material behavior value that is affecting the grain size directly.

Due to its good weldability, corrosion resistance and adequate high temperature mechanical properties, austenitic stainless steel (ASS) is used in different industries, such as petrochemical, shipbuilding, and nuclear industries. These steels are non-magnetic, stable at room temperature, and cannot be hardened by heat treatment [3, 4]. In recent years, significant contributions have been made to predict the grain behaviour of surface treated component rather than welded components using simulation software [5–7]. As a preliminary investigation towards grain behaviour of welded components using simulation software for welding process, material information is very important as grain behaviour is highly dependent on the material chemical composition. Different technique and models have been employed to simulate arc welding process with various physical phenomena was observed and predicted. H. Jamshidi have investigate the grain growth kinetics of SS304 to predict the grain size [8]. Investigation of grain size after Gas Metal Arc Welding on dissimilar material SS304 and SS316 (filler) has proven that alloy segregation and prolong cooling time also generate coarse austenite grain structures next to the sensitized region at the fusion zone, and it became weaker than the surrounding structure [9]. Thus, the prediction of the grain size will focus at the HAZ zone as it is the area adjacent to the weld that was heated high enough to affect its microstructure but not enough to melt it. By undergoing microstructural changes, the HAZ has different mechanical and physical properties than the weld and the adjacent base metal.

In this study, an attempt has been made to estimate the grain size at the HAZ of bead-on-plate using similar material SS316L for base plate and filler wire. Grain size of SS316L has been experimentally determined to obtain the preliminary modified kinetic constant (M_o) and initial grain size (G_o) of the said material. Then, a subroutine for MSC Marc/Mentat grain size calculation have been developed based on the average grain size in free grain growth algorithm.

2 Numerical Computational and FEM Simulation

2.1 Numerical Computation for Grain Growth Prediction.

The grain size behaviour of type 304 stainless steel in low cycle fatigue at elevated temperature was investigated by Yada based on the smooth specimens with various grain sizes [10]. As default the grain size calculation within MSC Marc/Mentat are based on Yada's model is more suitable for forming process as the temperature range is within the cold and hot forming region. As welding process temperature is at an elevated temperature higher than material melting temperature range, the yada grain size model is deem unsuitable for predicting the grain size of multi-layer welding process. However, the capability to use a different analytical modelling of grain growth is available by developing a grain size prediction subroutine integrated within MSC Marc/Mentat software. As such, there is a need to implement a new mathematical model to simulate this phenomenon. The mathematical model for low carbon stainless steel grain growth has been selected from [11–13]. Since the HAZ is heated to temperature approaching the solidus temperature of the alloy, many precipitates that are present in the base metal may dissolve. Carbides and nitrides are the most likely precipitate form in the HAZ of austenitic stainless steel [14, 15]. This preliminary investigation focuses on the grain growth in the absence of alloying elements/precipitates (free grain growth) as the welding process duration is short thus carbide precipitate didn't accumulate at the grain boundary [16–18].

General equation for grain growth.

$$\frac{\partial \overline{g}}{\partial t} = M_0^* \exp\left[-\frac{Q_{app}}{RT(t)}\right]\left[\frac{1}{\overline{g}} - \frac{1}{\overline{g}_{\lim}}\right]^{\left(\frac{1}{n}-1\right)} \tag{1}$$

where

M_0^* Modified kinetic constant ($\mu m^2 s^{-1}$).
Q_{app} Activation energy (kJ mol^{-1}).
R Gas constant (8314 J K^{-1} mol^{-1}).
T Absolute temperature (K).
$\overline{g}$ Average/initial grain size (μm).

The $\overline{g}_{\lim}$ value depends on the different cases.

The grain growth in the absence of alloying elements/precipitates (free grain growth),

where

r_0 Initial radius of precipitate (μm).
f_0 Initial volume fraction of precipitate.

$\overline{g}_{\lim} = \infty$, due to $\overline{g_{\lim}}^0 = k\frac{r_0}{f_0}$

Table 1 Data used for type predicting SS316L grain size

n	Q_{app} (kJ mol^{-1})	ΔH (kJ mol^{-1})	Q_d (kJ mol^{-1})	$\overline{D}_O$ (μm)	M_o (μm^2 s^{-1})
0.5**	224**,***	60**	240**	11.1*	2000×10^{9}**,***

*Value obtained from experiment; **Value obtained from miscellaneous sources; ***Value obtained from experiment and are temperature dependent

$$\frac{\partial \overline{g}}{\partial t} = M_0^* \exp\left[-\frac{Q_{app}}{RT(t)}\right]\left[\frac{1}{\overline{g}}\right]^{\left(\frac{1}{n}-1\right)} \tag{2}$$

The implementation of the mathematical model is established by writing a user subroutine to be used by the finite element analysis (FEA) software. The newly developed grain growth model based on the models of Zener, Hellman and Hillbert and Gladman estimate the limiting austenite grain size D_{lim} in the transformed parts of the weld HAZ when the oxygen and sulphur contents of the as-deposited weld metal are 0.04 and 0.01 wt%, respectively [7]. The grain growth model was suitable to be used as the material selected was the same category as type 316 austenitic stainless steel. The data used was compiled from miscellaneous source and experiment shown in Table 1.

Towards finding the material parameters of grain size for SS316L austenitic stainless steels, a series of experiment has been conducted. A series of experiment with different temperature range is needed to identify and verify the data used based on the raw material used for the investigation. Firstly, the specimens as shown in Fig. 1 had been through heat treatment process using DIL 805A/D quenching and deformations dilatometers. This regulated experiment controls the exposed temperatures for the heat treatment process were 1200 °C (peak temperature) with a holding time of 30 s. Afterwards an epoxy mount has been used for the specimens. After 12 h, the specimens were grinded by forcipol grinding machine. The specimens were polished for better surface texture. Then a metallographic observation was conducted, the specimens were etched with V2A solution for 10 min and consequently the grain size of the 316 stainless steel specimens were defined.

Fig. 1 SS316L specimens

2.2 FEM Simulation for Grain Growth Prediction on Bead-On-Plate Using MSC Marc/Mentat

The thermo-mechanical simulation of the welding process is applied using MSC MSC Marc/Mentat. The simulation is divided into 3 stages; preprocessing, solving and post-processing. The general flow of the simulation is displayed in Fig. 2, where the first seven stages are preprocessing followed by solving and post processing. The chosen type of meshing is quad-mesh due to the geometric shape of the work piece to be relatively simplified. Since not much strain and change of shape is expected, using simplified mesh is done to save computing time and ease the modelling effort.

2.2.1 Geometrical Modelling

A schematic illustration of Finite Element (FE) models of bead on plate is displayed in Fig. 3. To build the model as accurate as possible the entire FE model of bead on plate components consists of a table (rigid solid), the substrate material (60 mm × 140 mm × 4 mm) and weld beads was developed. A rectangular-shape model of 90 mm of length along with 6 mm in width was modelled as weld filler. Simulating the experiment, the welding trajectory is located at the upper layer of the base plate. The location and forces of the clamping conditions is important to be as identical to the experiment also has been included in the simulation. This is important as clamping conditions such as clamping location, clamping forces and clamping connection has

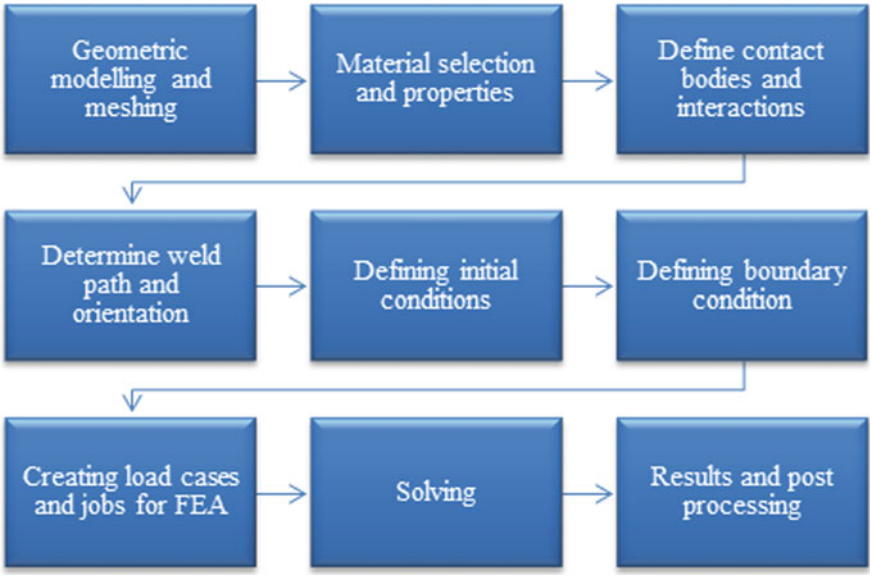

Fig. 2 General flowchart of simulation procedure using MSC Marc/Mentat [19]

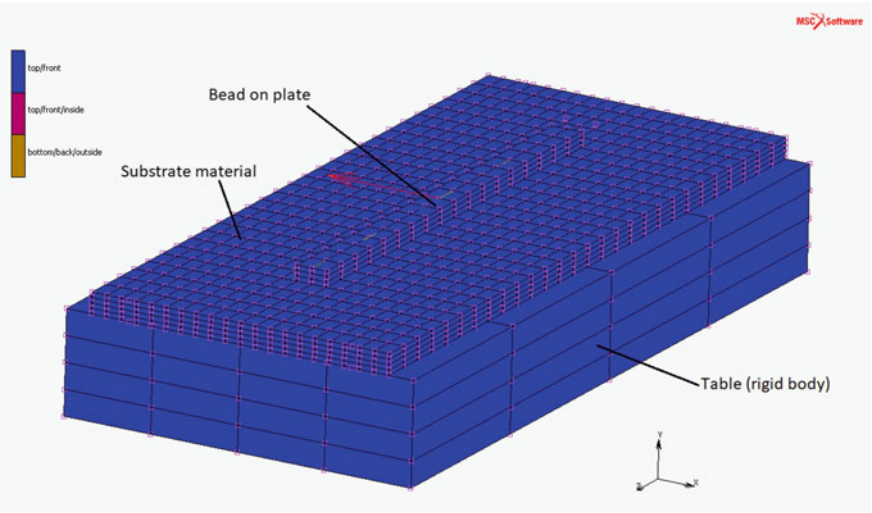

Fig. 3 FEM geometrical modelling

been previously studied will affect the distortion value of multi layered welding process [20, 21]. Finer elements also have been considered along the welding HAZ for research purposes.

2.2.2 Material Characterisation and Modelling

SS316L Stainless Steel has been used as the filler material, and the base plate material to predict the grain size. The chemical composition of the plate was analysed by Arc Spectrometer (Q4 Qantas) as stated in Table 2. In this simulation both thermo-physical and thermo-mechanical material properties should be imported into FEM simulation using existing database from the software library, but as SS316L material wasn't in the default database, it has been added manually by using JMATPro software by using the chemical composition obtained from the physical experiment.

The mechanical and physical properties are as presented in Table 3.

Table 2 QMatrix analysis results for SS316L stainless steel plate (wt%)

C	Si	Mn	P	S	Ni	Cr	Mo	Fe
0.017	0.340	1.475	0.026	0.069	10.19	16.76	2.148	68.44

Table 3 Mechanical and physical properties of SS316L

Properties	Values
Yield strength (MPa)	25,000
Ultimate tensile strength (Mpa)	70,000
Poisson's ratio (V)	0.275
Melting range (°C)	1390–1440
Modulus of elasticity (GPa)	200

Table 4 Welding parameters

Welding parameters	Value
Current, I (A)	172
Voltage, V (V)	20
Travel speed, v (mm/s)	5.0

2.2.3 Welding Parameter and Heat Source Model

Table 4 displays the parameters which are implemented on the commercial software MSC Marc/Mentat. Therefore, the Current (I) and the Voltage (V) are considered under the power equation. The assigned travel speed was based on the experimental welding speed to have a more accurate model.

In a welding simulation using FEM, an important factor to be considered is the heat source model. The Goldak double ellipsoid model is mostly used as the heat source model in a typical simulation of an arc welding process as in Fig. 4. This is due to its accuracy and reliability in representing the shape and distribution of the heat flux proposed by Goldak et al. [22]. The heat input model is by no mean constrained to the double ellipsoid. A thorough description of this heat source model

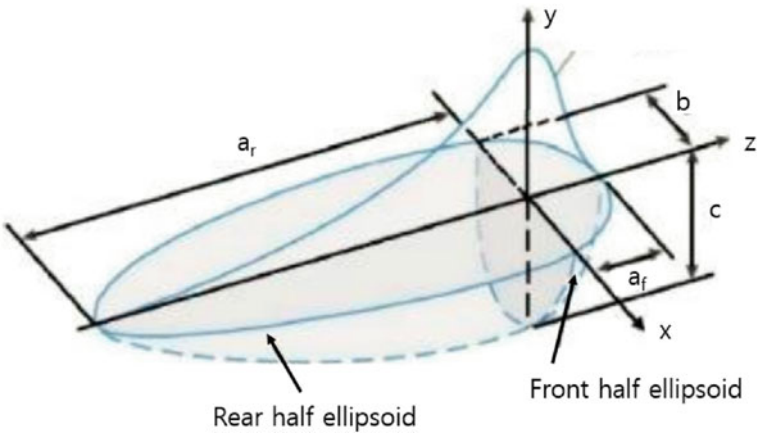

Fig. 4 Goldak's double ellipsoid heat. *Source* model

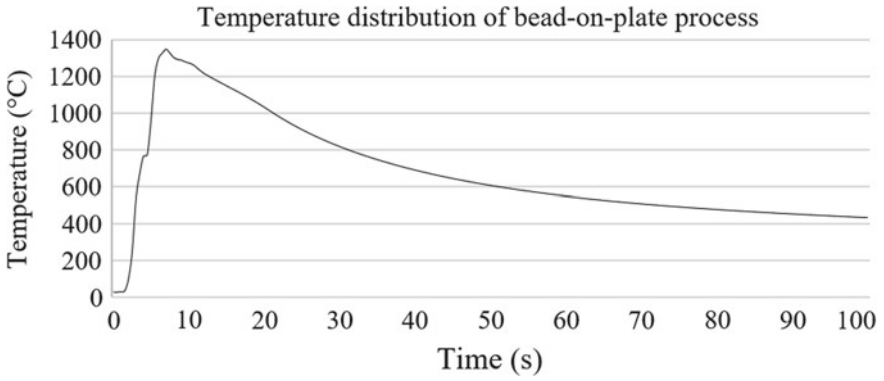

Fig. 5 Bead on plate temperature distribution

can be found in [23]. The schematic of the heat source model is shown in Fig. 4. The heat source parameters were obtained from previous studies [24].

3 FEM Simulation on Bead-On-Plate

3.1 Temperature Distribution

Temperature distribution of bead-on-plate process is presented in Fig. 5. The temperature by previous studies suggest that the cooling time from peak temperature until 900 °C of the welding process is the most influential temperature for grain size transformation [25, 26]. However, the grain size transformation has been calculated successfully by implementing a numerical model for predicting the grain size transformation for various temperature specifically to understand the grain growth behavior of austenitic stainless steel SS316L.

4 Results and Discussion

Grain size prediction using the numerical model has been conducted successfully for various temperature range is shown in Table 5. The selected temperature for initial temperature and final temperature were selected from previous studies related to grain growth in welds.

Comparing the grain size in from the table above, it can be obtained that as the material exposure to heat input increases with time the influence on grain size is more obvious. The most preferable model will be from the peak temperature until 900 °C as the error percentage is within the acceptable range. As many previous

Table 5 Grain size prediction

Initial temperature (°C)	Final temperature (°C)	Final grain size (μm)	Experimental grain size (μm)	Error percentage (%)
Peak temperature (highest)	900	25.6	23.2	10.34
Peak temperature (highest)	500	30.2		30.17
Peak temperature (highest)	Cooling temperature	38.8		67.24
($T_{8/5}$) 800	500	16.5		28.2

researchers before indicating that the austenitic stainless steel grain growth rate will increase rapidly with time and temperature but the short exposure time of elevated temperature due to the selected bead-on-plate process has limit the opportunity of the austenitic stainless steel to grow. At peak temperature range to cooling temperature provides ample time for the grains to grow up, thus the grains size has obviously increased. As alloying elements are added in the carbon steels, the grain growth rate usually decreases due to the solute dragging effect of the alloying elements segregated into austenite grain boundaries. If the alloying elements precipitate as carbides or nitrides in austenite, the precipitates also lower the grain growth rate by pinning the grain boundaries. The result from the selected temperature of $T_{8/5}$ from previous studies shows also a low error percentage, as the low carbon content in SS316L didn't permit the grain size to increase with enough time within the time range. Grain coarsening will lead to adverse effects such as strength reduction, so it is important to avoid significant grain grow in welding process. It is important to note that as reported by Shu Xin and Shaoying, no chromium carbide was observed after 100 h of 650 °C temperature exposure of heat treatment, this indicate that the austenitic stainless steel with low carbon content [27, 28].

5 Conclusions

The main objectives of this research are to analyse the capability of MSC/Marc Mentat FEM software with integrated subroutine in predicting the final grain size of multi-layer welding process. The success of this basic investigation for bead-on-plate process will allow the further step of predicting additive manufacturing component grain size using the same material but within a more complex temperature environment such as wire arc additive manufacturing (WAAM). Thus, the prediction of the final grain size allows the prediction of the material strength even before the fabrication occur to save time and cost. As WAAM is becoming more preferred choice for fabrication due to its higher deposition rate suitable for bigger structure, investigating the capability of FEM software to support the prediction of the material

strength for additive manufactured component will be an advantage for engineers and the industry. As conclusion, following contributions can be summarized.

1. The numerical analysis for bead-on-plate process final grain size of SS316L filler wire and substrate material at the HAZ has been successfully executed.
2. The simplified bead model in rectangular form will allow reduction of the computational time.
3. The well-known Goldak's double ellipsoid heat source model can be improved for rectangular mesh geometry to simulate multi-pass welding or additive manufacturing.
4. The difference in temperature result might be resulted due to material inhomogeneity, parameters fluctuations etc.

As further recommendations, following suggestions are to be proposed:

1. Rectangular heat source models should be investigated to reduce the computational time while maintaining an acceptable value of percentage error.

Other material final grain size model should be explored within the same category and compared to better understand the austenitic stainless-steel grain growth behaviour.

Acknowledgements The authors would like to express their gratitude to staff member of Smart Manufacturing Research Institute (SMRI) as well as Research Interest Group: Advanced Manufacturing Technology (RIG:AMT) and Advanced Manufacturing Technology Excellence Centre (AMTEx) at Faculty of Mechanical Engineering, Universiti Teknologi MARA (UiTM) for encouraging this research. This research and conference participation are also financially supported by ASEA-UNINET grant with the project number ASEA 2019/Montan/1, ERASMUS+ (Montan University in Leoben) and Technogerma Engineering & Consulting Sdn. Bhd.

References

1. Lewandowski JJ, Seifi M (2016) Metal additive manufacturing: a review of mechanical properties. Annu Rev Mater Res
2. Taiwade RV, Shukla R, Vashishtha H, Ingle AV, Dayal RK (2014) Effect of grain size on degree of sensitization of chrome-manganese stainless steel. ISIJ Int 53(12):2206–2212
3. Zhang Y, Liu F, Chen J, Yuan Y (2017) Effects of surface quality on corrosion resistance of 316L stainless steel parts manufactured via SLM. J Laser Appl
4. Mohammad Soltani H, Tayebi M (2018) Comparative study of AISI 304L to AISI 316L stainless steels joints by TIG and Nd:YAG laser welding. J Alloys Compd 767:112–121
5. Zhao X, Liu Y, Wang, YAN, Feng P, Tang H (2014) Recrystallization and grain growth of 316L stainless steel wires
6. Khalaj MTG, Yoozbashizadeh H, Khodabandeh A (2014) Austenite grain growth modelling in weld heat affected zone of Nb/Ti microalloyed linepipe steel. Mater Sci Technol 30(4):424–433
7. Moon J, Lee J, Lee C (2007) Prediction for the austenite grain size in the presence of growing particles in the weld HAZ of Ti-microalloyed steel. Mater Sci Eng A
8. Jamshidi Aval H, Serajzadeh S, Kokabi AH (2009) Prediction of grain growth behavior in haz during gas tungsten arc welding of 304 stainless steel. J Mater Eng Perform

9. Tasalloti H, Kah P, Martikainen J (2014) Effects of welding wire and torch weaving on GMAW of S355MC and AISI 304L dissimilar welds. Int J Adv Manuf Technol
10. Okazaki M, Yada T, Endoh T (1989) Surface small crack growth behavior in low-cycle fatigue at elevated temperature and application limit of macroscopic crack growth law. Nucl Eng Des
11. Andersenj I, Grong O (1995) Analytical modelling of grain growth in metals and alloys in the presence of growing and dissolving precipitates. Normal Grain Growth 43(7):2673–2688
12. Grong Ø (1997) Metallurgical modelling of welding, 2nd edn. The Institute of Materials
13. Akselsen OM, Grong NR, Christensen N (1986) HAZ grain growth mechanisms in welding of low carbon microalloyed steels. Acta Metall 34(9):1807–1815
14. Lippold JC, Kotecki DJ (2005) Welding metallurgy and weldability of stainless steel. John Wiley, Hoboken, NJ
15. DuPont JN, Lippold JC, Kiser SD (2009) Welding metallurgy and weldability of nickel-base alloys
16. Sarkari Khorrami M, Mostafaei MA, Pouraliakbar H, Kokabi AH (2014) Study on microstructure and mechanical characteristics of low-carbon steel and ferritic stainless steel joints. Mater Sci Eng A 608:35–45
17. Hong HU, Nam SW (2002) The occurrence of grain boundary serration and its effect on the M23C6 carbide characteristics in an AISI 316 stainless steel. Mater Sci Eng A
18. Wasnik DN, Dey GK, Kain V, Samajdar I (2003) Precipitation stages in a 316L austenitic stainless steel. Scr Mater 49(2):135–141
19. Yahya O, Manurung YHP, Sulaiman MS, Keval P (2018) Virtual manufacturing for prediction of martensite formation and hardness value induced by laser welding process using subroutine algorithm in MSC Marc/Mentat 15(2):107–125
20. Montevecchi F, Venturini G, Scippa A, Campatelli G (2016) Finite element modelling of wire-arc-additive-manufacturing process. Proc CIRP
21. Ganesh KC, Vasudevan M, Balasubramanian KR, Chandrasekhar N, Vasantharaja P (2014) Thermo-mechanical analysis of TIG welding of AISI 316LN stainless steel. Mater Manuf Process
22. Goldak J, Chakravarti A, Bibby M (1984) A new finite element model for welding heat sources. Metall Trans B
23. Lindgren LE (2007) Computational welding mechanics: thermomechanical and microstructural simulations
24. Hou ZB, Komanduri R (2000) General solutions for stationary/moving plane heat source problems in manufacturing and tribology. Int J Heat Mass Transf 43(10):1679–1698
25. Choi J, Mazumder J (2002) Numerical and experimental analysis for solidification and residual stress in the GMAW process for AISI 304 stainless steel. J Mater Sci
26. Wang Y, Ding M, Zheng Y, Liu S, Wang W, Zhang Z (2016) Finite-element thermal analysis and grain growth behavior of HAZ on argon tungsten-arc welding of 443 stainless steel. Met (Basel)
27. Li SX, He YN, Yu SR, Zhang PY (2013) Evaluation of the effect of grain size on chromium carbide precipitation and intergranular corrosion of 316L stainless steel. Corros Sci 66:211–216
28. Li S et al (2018) Carbide precipitation during tempering and its effect on the wear loss of a high-carbon 8 Mass% Cr tool steel. Mater (Basel) 11(12)